Quantitative Imaging of Single, Unstained Viruses with Coherent X Rays

Changyong Song,[1] Huaidong Jiang,[1] Adrian Mancuso,[1] Bagrat Amirbekian,[1] Li Peng,[2] Ren Sun,[2] Sanket S. Shah,[3] Z. Hong Zhou,[4] Tetsuya Ishikawa,[5] and Jianwei Miao[1,*]

[1]*Department of Physics and Astronomy, University of California, Los Angeles, California 90095, USA*
[2]*Department of Molecular and Medical Pharmacology, University of California, Los Angeles, California 90095, USA*
[3]*Department of Pathology and Laboratory Medicine, University of Texas-Houston Medical School, Texas 77030, USA*
[4]*Department of Microbiology, Immunology & Molecular Genetics, University of California, Los Angeles, California 90095, USA*
[5]*RIKEN SPring-8 Center, 1-1-1, Kouto, Sayo, Hyogo 679-5148, Japan*
(Received 8 July 2008; revised manuscript received 18 September 2008; published 7 October 2008)

We report the recording and reconstruction of x-ray diffraction patterns from single, unstained viruses, for the first time. By separating the diffraction pattern of the virus particles from that of their surroundings, we performed quantitative and high-contrast imaging of a single virion. The structure of the viral capsid inside a virion was visualized. This work opens the door for quantitative x-ray imaging of a broad range of specimens from protein machineries and viruses to cellular organelles. Moreover, our experiment is directly transferable to the use of x-ray free electron lasers, and represents an experimental milestone towards the x-ray imaging of large protein complexes.

Since Perutz, Kendrew, and colleagues unveiled the structure of hemoglobin and myoglobin based on x-ray diffraction analysis in the 1950s [1,2], x-ray crystallography has become the primary methodology used to determine the 3D structure of macromolecules. However, biological specimens such as cells, organelles, some viruses, and many important macromolecules are difficult or impossible to crystallize, and hence their structures are not accessible by crystallography. Overcoming this major limitation requires the employment of different techniques. One promising approach currently under rapid development is x-ray diffraction microscopy (or coherent diffractive imaging) where the x-ray diffraction patterns of noncrystalline specimens are measured and then directly phased by the oversampling iterative algorithm [3]. However, due to the absence of the very large signal amplification that occurs in crystals, x-ray diffraction microscopy has so far been limited to the imaging of micron-sized or high-Z specimens [4–19].

Here we, for the first time, recorded and reconstructed x-ray diffraction patterns from single, unstained viruses that have molecular mass about 3 orders of magnitude smaller than those specimens investigated by x-ray diffraction microscopy before. By separating the diffraction pattern of the virus particles from that of their surroundings, we performed quantitative and high-contrast imaging of a single virion with a resolution of 22 nm. The structure of the viral capsid inside the virion was identified. With more brilliant synchrotron radiation sources [20] and future x-ray free electron lasers (X-FELs) [21], much higher resolutions should be achievable. Because of its quantitative capability, high image contrast, and high spatial resolution, we anticipate that x-ray diffraction microscopy will become an important imaging technique for unveiling the structure of a broad range of biological systems including single protein machineries, viruses, organelles, and whole cells.

The samples we studied are single murine herpesvirus-68 (MHV-68) virions. A herpesvirus virion has an asymmetric tegument and envelope outside of the icosahedrally symmetric capsid composed of defined numbers of subunits [22]. However, each virion may have a different size of tegument and envelope, and the viral capsid is not necessary in the center of the virion [23]. While cryoelectron microscopy can determine the capsid structure of herpesviruses by averaging over thousands of virus particles [24], the reconstructions of pleomorphic virions obtained by cryoelectron tomography are limited in low image contrast and high levels of noise [23]. The goal of this study is to perform quantitative and high-contrast imaging of single, unstained virions by using coherent x rays. The MHV-68 virions were inactivated by UV light (500 mJ) and chemically fixed by 3% glutaraldahyde. Unstained virions were suspended in methanol to regulate the concentration to about 20 virions/μL and supported on 30-nm thick silicon-nitride-membranes. Single, isolated virions were located with a high-resolution optical microscope and studied by the x-ray diffraction microscope.

The experiment was carried out on an undulator beam line at SPring-8. Figure 1 shows the schematic layout of the biological x-ray diffraction microscope. Unfocused, monochromatic x rays with an energy of 5 keV were filtered by a 20 μm-diameter-pinhole, placed approximately 1 m upstream of the sample. A Si guard slit with beveled edges was positioned just in front of the sample to block the parasitic scattering from the upstream optical components. Coherent x-ray diffraction patterns were recorded by a liquid-nitrogen-cooled CCD camera with 1340×1300
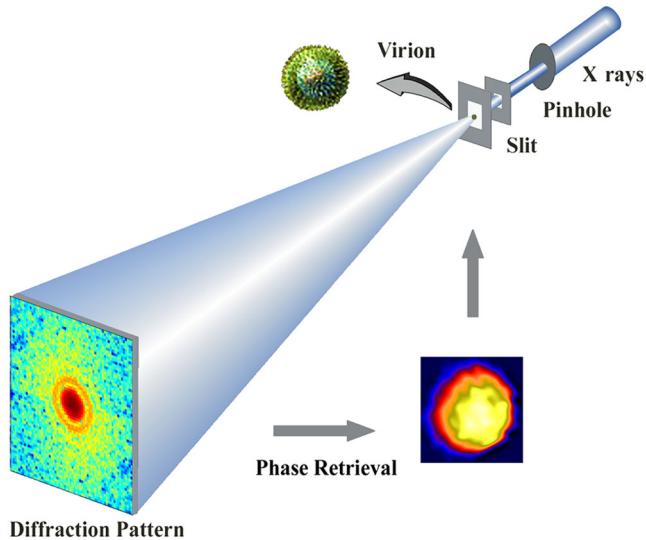
FIG. 1 (color online).   Schematic layout of the x-ray diffraction microscope. A 20-um pinhole was used to define the incident x-ray beam. The virion specimen was positioned at a distance of 1 m from the pinhole. A silicon guard slit with beveled edges was used to eliminate the parasitic scattering from the pinhole. The oversampled diffraction pattern, recorded on a liquid-nitrogen-cooled CCD camera, was directly inverted to a high-contrast image using an iterative algorithm.
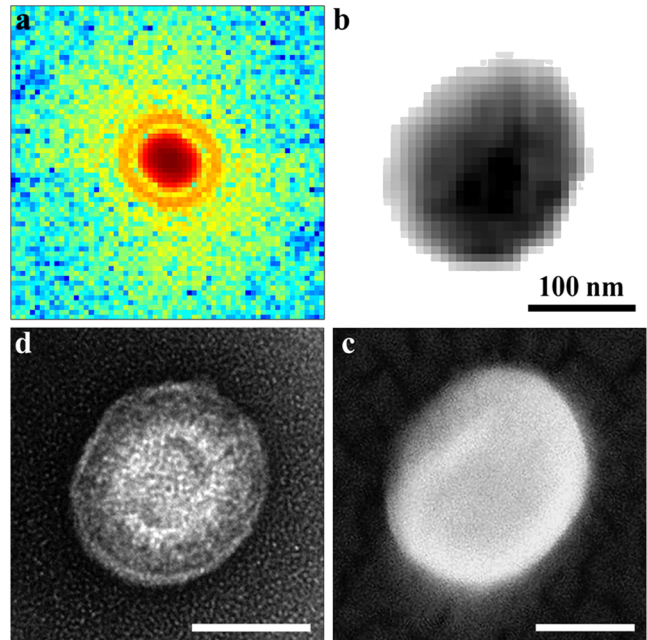

FIG. 2 (color online).   X-ray diffractive imaging of single herpesvirus virions. (a) X-ray diffraction pattern obtained from a single, unstained virion. (b) High-contrast image reconstructed from (a) where the background and the surroundings of the virion were completely removed. (c) SEM image of the same virion. (d) Negative stain TEM image of a similar herpesvirus virion.

pixels and a pixel size of 20 μm, located a distance of 1 m downstream of the sample. To obtain the diffraction pattern only from single virions, we measured two sets of diffraction intensities with the specimens in and out of the x-ray illumination, and then subtracted the two diffraction patterns. This procedure removed the unwanted scattering from specimens' surroundings and allowed us to perform quantitative and high-contrast imaging of single virions. The resolution of the diffraction pattern was estimated to be 22 nm based on q_{max} of the diffracted signal.

Figure 2(a) shows the diffraction pattern of a single, unstained virion which was added up from three independent diffraction patterns, each having a radiation dose of $\sim 3.5 \times 10^7$ Gy. Careful examination of the three diffraction patterns indicated that the radiation dose made minimum appreciable structure changes to the virion at this resolution. To significantly improve the signal-to-noise ratio (SNR) of the diffraction pattern, we integrated the diffraction intensities by binning 13×13 pixels into 1 pixel, and performed deconvolution to the integrated pattern [25]. The deconvolution process removed the effects of the finite pixel size of the CCD on the phase retrieval [25]. Figure 2(a) shows the characteristic ring structures of the diffraction pattern, reflecting the general round shape of the virion. Based on the diameter of the rings, the size of the virion was estimated to be ~ 200 nm. Intensity variation along the azimuthal angle is also visible in Fig. 2(a), which is due to the internal structure of the virion.

The phase retrieval of the diffraction pattern was carried out by the guided hybrid-input-output algorithm (GHIO) [14,26]. The GHIO started with 16 independent reconstructions of the diffraction pattern with different random phase sets as the initial input. Each reconstruction was iterated back and forth between real and reciprocal space while positivity and zero-density constraints were enforced. The iterative algorithm was guided towards minimizing the R value, i.e., the difference between the measured and calculated Fourier modulus. The algorithm was terminated when the R value could not be further improved and all the 16 independent reconstructions became very consistent. Figure 2(b) shows the average of the five best images with the smallest R values. To examine the reliability of the reconstruction, we performed another GHIO run of the x-ray diffraction pattern. Figures 3(a) and 3(b) show the final images from two independent GHIO runs. The reconstruction error (R_{err}) was calculated by

$$R_{err} = \frac{\sum_{x,y} |\rho_1(x, y) - \rho_2(x, y)|}{\sum_{x,y} |\rho_1(x, y) + \rho_2(x, y)|}, \qquad (1)$$

where $\rho_1(x, y)$ and $\rho_2(x, y)$ represent the two final reconstructed images. R_{err} between Figs. 3(a) and 3(b) was estimated to be $\sim 2.3\%$, indicating the robustness of the phase retrieval. We also took a scanning electron microscopy (SEM) image of the same virion [Fig. 2(c)], on which
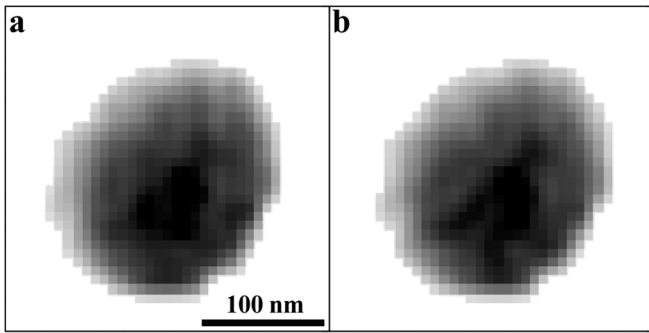
FIG. 3.   (a),(b) The final reconstructed images from two inde-
pendent GHIO runs. Each image was obtained by averaging the
five best images with the smallest R values.

a 5 nm thick Au film was deposited to remove the surface
charging effect. While the SEM image only provides the
surface morphology of the virion, the overall shape is in
good agreement with the x-ray image. To characterize the
internal structure, we took negative stain TEM images of
similar virions, shown in Fig. 2(d). The bright circular
region in the TEM image represents the viral capsid which
is tightly packed of the viral genome. The high-density
region in the x-ray image [i.e., the darker area in Fig. 2(b)]
shows features similar to the capsid structure of the TEM
image. Compared with the thin-film-deposited SEM and
negative stain TEM images, the x-ray diffraction image of
a single, unstained virion shows the highest contrast as the
background and surroundings of the virion were com-
pletely removed.

   To quantify the x-ray image, we calculated the absolute
electron density of the virion by

$$I(0, 0) = I_0 r_e^2 |F(0, 0)|^2 \frac{\Delta s}{r^2}, \qquad (2)$$

where $I(0, 0)$ represents the number of diffracted x-ray
photons in the forward direction (i.e., within the centro-
pixel of the CCD camera), I_0 is the incident x-ray flux per
unit area, r_e is the classical electron radius, $|F(0, 0)|$ rep-
resents the total number of electrons in the virion, Δs is the
area of the centropixel, and r is the distance from the
sample to the CCD camera. Although $I(0, 0)$ cannot be
experimentally measured due to a beam stop, our recent
results have shown that as long as the missing data are
confined within the centrospeckle, they can be reliably
recovered from the measured diffraction intensities alone
[27]. Figure 4(a) shows the absolute electron density of the
virion, where the yellow region represents the highest
electron density with a size of ∼100 nm. Figure 4(b)
shows an AFM image of a similar virion, which was
used to estimate the thickness profile of the virions. After
taking the thickness into account, the electron density
within the contour line was estimated to be approximately
1.3 times higher than the average density of the virion. It is
reasonable to conclude that the high-density region repre-
sents the viral capsid of the single, unstained virion. To
quantify the contrast of the viral capsid, we took a lineout
across the capsid shown in Fig. 5. Because of the high-
contrast ability of the x-ray diffraction microscope, the
absolute electron density variations inside the capsid are
visible (Fig. 5), which may be due to the packing of the
viral genome.

   Presently, the resolution of x-ray diffraction microscopy
is limited by the coherent x-ray flux. With more brilliant
synchrotron radiation sources [20], the resolution is ulti-
mately limited by radiation damage to biological speci-
mens [28,29]. While cryogenic cooling of biological speci-
mens can alleviate the radiation damage problem [30–32],
recent studies have shown that the highest resolution at-
tainable for imaging the 3D pleomorphic structure of bio-
logical specimens is ∼5 nm [28,29]. For the imaging of
large protein molecules having identical copies, the reso-
lution may be further improved by employing extremely
intense and ultrafast x-ray pulses such as X-FELs [21].
Computer modeling and experimental results have both in-
dicated that significant damage occurs only after an ultra-
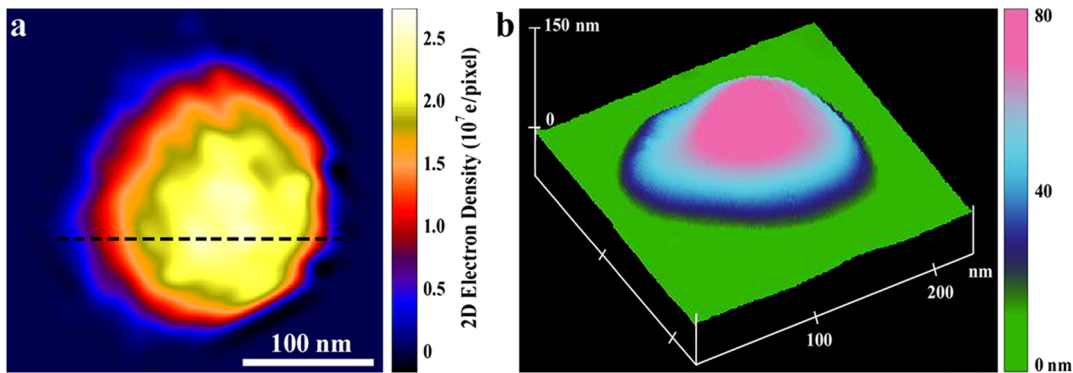fast x-ray pulse (≤25 fs) traverses a specimen [13,34]. By

FIG. 4 (color online).   (a) Quantitative characterization of the reconstructed electron density map of the herpesvirus virion. The
dashed line was used to obtain the lineout shown in Fig. 5. (b) AFM image of a similar virion, showing the thickness profile of a similar
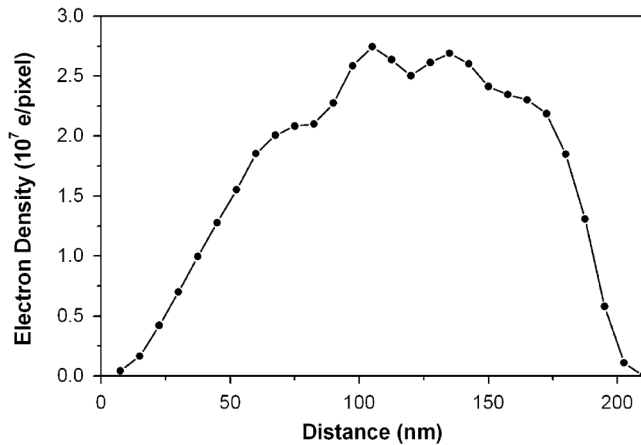virion.

FIG. 5.   Lineout across the viral capsid [i.e., along the dashed line in Fig. 4(a)], showing the distribution of the absolute electron density. The density variations inside the capsid may be due to the packing of the viral genome.

using computer simulations, it has been shown that approximately 10^5–10^6 identical copies of single large protein (i.e., molecular mass >100 kDa) can lead to the 3D structure of the molecules at the near atomic resolution [34].

In summary, coherent x-ray diffraction patterns were obtained from a single, unstained herpesvirus virion, and then directly inverted to yield quantitative and high-contrast electron density maps with a resolution of 22 nm. The quantitative structure of the viral capsid inside the virion was visualized. While the present resolution is limited by the coherent x-ray flux, higher resolutions should be achievable by using more brilliant synchrotron radiation sources [20]. This work hence opens the door for broad application of x-ray diffraction microscopy to biological specimens ranging from single large protein machineries, viruses and cellular organelles to whole cells. As tabletop soft x-ray diffraction microscopy based on the high harmonic generation and soft x-ray laser sources has recently been demonstrated [17,18], the combination of this work with compact x-ray sources will make this imaging technique more accessible to the biology community. Finally, X-FELs are undergoing rapid development worldwide [21]. Arguably, the major driving force for these large-scaled coherent x-ray sources is the potential of imaging single biomolecules. The first recording and reconstruction of x-ray diffraction patterns from single, unstained virions hence represents an experimental milestone towards the ultimate goal of imaging large protein complexes [33,34].

*Corresponding author.
miao@physics.ucla.edu.

[1]   M. F. Perutz *et al.*, Nature (London) **185**, 416 (1960).
[2]   J. C. Kendrew *et al.*, Nature (London) **181**, 662 (1958).
[3]   J. Miao, T. Ishikawa, T. Earnest, and Q. Shen, Annu. Rev. Phys. Chem. **59**, 387 (2008).
[4]   J. Miao, P. Charalambous, J. Kirz, and D. Sayre, Nature (London) **400**, 342 (1999).
[5]   I. K. Robinson *et al.*, Phys. Rev. Lett. **87**, 195505 (2001).
[6]   J. Miao *et al.*, Phys. Rev. Lett. **89**, 088303 (2002).
[7]   G. J. Williams *et al.*, Phys. Rev. Lett. **90**, 175501 (2003).
[8]   J. Miao *et al.*, Proc. Natl. Acad. Sci. U.S.A. **100**, 110 (2003).
[9]   S. Marchesini *et al.*, Phys. Rev. B **68**, 140101 (2003).
[10]   D. Shapiro *et al.*, Proc. Natl. Acad. Sci. U.S.A. **102**, 15343 (2005).
[11]   M. A. Pfeifer *et al.*, Nature (London) **442**, 63 (2006).
[12]   H. M. Quiney *et al.*, Nature Phys. **2**, 101 (2006).
[13]   H. N. Chapman *et al.*, Nature Phys. **2**, 839 (2006).
[14]   J. Miao *et al.*, Phys. Rev. Lett. **97**, 215503 (2006).
[15]   G. J. Williams *et al.*, Phys. Rev. Lett. **97**, 025506 (2006).
[16]   J. M. Rodenburg *et al.*, Phys. Rev. Lett. **98**, 034801 (2007).
[17]   R. L. Sandberg *et al.*, Phys. Rev. Lett. **99**, 098103 (2007).
[18]   R. L. Sandberg *et al.*, Proc. Natl. Acad. Sci. U.S.A. **105**, 24 (2008).
[19]   B. Abbey *et al.*, Nature Phys. **4**, 394 (2008).
[20]   www.diamond.ac.uk; www.bnl.gov/nsls2; http://petra3. desy.de/; http://ssrf.sinap.ac.cn.
[21]   www-ssrl.slac.stanford.edu/lcls; www-xfel.spring8.or.jp; http://xfel.desy.de.
[22]   A. C. Steven and P. G. Spear, *Herpesvirus Capsid Assembly and Envelopment in Structural Biology of Viruses*, edited by W. Chiu, R. M. Burnett, and R. Garcea (Oxford University Press, New York, 1997), pp. 312–351.
[23]   K. Grunewald *et al.*, Science **302**, 1396 (2003).
[24]   H. Zhou *et al.*, Science **288**, 877 (2000).
[25]   C. Song *et al.*, Phys. Rev. B **75**, 012102 (2007).
[26]   C. C. Chen, J. Miao, C. W. Wang, and T. K. Lee, Phys. Rev. B **76**, 064113 (2007).
[27]   J. Miao *et al.*, Phys. Rev. Lett. **95**, 085503 (2005).
[28]   Q. Shen, I. Bazarov, and P. Thibault, J. Synchrotron Radiat. **11**, 432 (2004).
[29]   M. R. Howells *et al.*, J. Electron Spectrosc. Relat. Phenom. (to be published).
[30]   J. Kirz, C. Jacobsen, and M. R. Howells, Q. Rev. Biophys. **28**, 33 (1995).
[31]   G. Schneider, Ultramicroscopy **75**, 85 (1998).
[32]   J. Maser *et al.*, J. Microsc. **197**, 68 (2000).
[33]   R. Neutze *et al.*, Nature (London) **406**, 752 (2000).
[34]   J. Miao, K. O. Hodgson, and D. Sayre, Proc. Natl. Acad. Sci. U.S.A. **98**, 6641 (2001).